Chapter 2

LITERATURE REVIEW

Jaky's formula was often used to calculate the earth pressure at-rest behind a retaining wall. However, the theory to estimate the lateral earth pressure on retaining wall near an inclined rock face has received very little attention in the literature. Theoretical and empirical relationship to estimate the lateral earth pressure adjacent to a vertical rock face has been reported by Janssen (1895), Reimbert and Reimbert (1976), and Spangler and Handy (1984) articles mentioned above will be discussed in this chapter.

2.1 Earth Pressure At-Rest

2.1.1 Coefficient of Earth Pressure At-Rest

In Fig.2.1(a), the soil element A formed in a horizontal sedimentary deposit is compressed by the overburden pressure $\sigma_v = \gamma z$. During the formation of the deposit, the element is consolidated under the pressure σ_v. The vertical stress tends to produce a lateral deformation against surrounding soils due to the Poisson's ratio effect. However, the surrounding soil resists the lateral deformation with a developed lateral stress σ_h. Over the geological period, the horizontal strain is kept to be zero. A stable stress state will develop in which the principal stresses σ_1 and σ_3 acts on the vertical and horizontal planes, as shown Fig.2.1(b). The equilibrium condition produced at this stress in commonly termed as the K_o condition. The ratio of the horizontal stress σ_h to vertical stress σ_v is defined as the coefficient of earth pressure at-rest, K_o, or

$$K_o = \frac{\sigma_h}{\sigma_v} \qquad (2.1)$$

since $_v = z$, then $\sigma_h = K_0 \gamma z$, where γ is the unit weight of soil.

2.1.2 Jaky's Formula

Attempts have been made to establish a theoretical relationship between the strength properties of a soil and the coefficient K_o. The empirical relationship to estimate K_o of coarse-grained soils is discussed in this section. Mesri and Hayat (1993) reported that Jaky (1944) arrived at the relationship between K_o and the internal friction angle ϕ by analyzing a talus of granular soil freestanding at the angle of repose. Jaky assumed that the angle of repose is equal to the internal friction angle ϕ. This is a reasonable assumption for sediment, normally consolidated materials. Jaky reasoned that the sand cone OAD illustrated in Fig.2.2 is in a state of equilibrium and its surface and inner points are motionless. The horizontal pressure acting on the vertical plane OC is the earth pressure at rest. Slide planes exist in the inclined sand mass. However, as OC is a line of symmetry, shear stresses cannot develop on it. Hence OC is a principal plane. Based on the equations of equilibrium, Jaky was able to expressed the coefficient of earth pressure at rest K_o with the angle of internal friction ϕ:

$$K_o = (1 - \sin\phi) \frac{1 + \frac{2}{3}\sin\phi}{1 + \sin\phi} \qquad 2.2$$

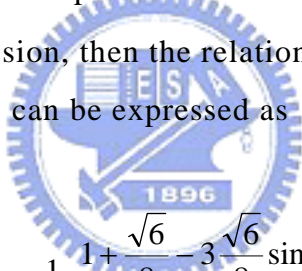without any further explanation Jaky (1944), adopted

$$K_0 = 1 - \sin\phi \qquad (2.3)$$

Mayne and Kulhawy (1982) reported that, the approximate theoretical

relationship for K_o for normally consolidated soils introduced by Jaky appears valid for cohesionless soils. Using Jaky's equation to estimate the in situ lateral earth pressure is reliable enough for most engineering purposes.

2.1.3 Hendron's Formula

Hendron (1963) reported a comprehensive study on the behavior of sand in one-dimensional compression. He derived a theoretical approach to predict K_o analytically. Hendron (1963) concluded that the values of K_o for round sand are lower than for an angular one at identical values of the angle of shearing resistance. The theoretical derivation of Hendron is based on the assumption that uniform, well-rounded, dense sand can be approximated by a face-centered array of equiradii spheres. If the array of spheres were subjected to one-dimensional compression, then the relationship between K_o and internal friction angle of the soil ϕ can be expressed as

$$K_o = \frac{1}{2}\left(\frac{1+\dfrac{\sqrt{6}}{8}-3\dfrac{\sqrt{6}}{8}\sin\phi}{1-\dfrac{\sqrt{6}}{8}+3\dfrac{\sqrt{6}}{8}\sin\phi}\right) \tag{2.4}$$

2.1.4 Study of Sherif, Fang and Sherif

Sherif, Fang and Sherif (1984) presented their experimental results regarding the at-rest stresses against a rigid wall as a function of soil density. All experiments were conducted in the University of Washington shaking table and retaining wall facility. The model system consists of four components: (1) shaking table and soil box; (2) loading and control units; (3) retaining wall; and (4) data acquisition system.

The shaking table is 3 m long, 2.4 m wide, 0.194 m deep, and is made of steel as shown in Fig. 2.3. A rigid soil box of 2.4 m long, 1.8 m wide and 1.2

m high is built on the shaking table for geotechnical earthquake engineering research. The movable model retaining wall and its driving system are shown in Fig. 2.4. The model wall consists of the main frame and the center wall. The center wall is 1 m wide, 1 m high, and 0.127 m thick. Six soil pressure transducers are mounted on the centerline of the wall surface at different depths (Fig. 2.5) to measure the soil pressure distribution against the main body of the center wall.

Figs. 2.6, 2.7 and 2.8 show the magnitudes and distribution of static at-rest stresses against the retaining wall for loose, medium dense and dense sand. The data in these figures reveal that the at-rest stress distribution behind non-yielding wall is linear. Fig. 2.6 indicates that the earth pressure distribution for loose sand in good agreement with the Jaky's equation. However, when the backfill behind the wall is either compacted or vibrated, the magnitude of the at-rest stresses increases as a result of densification of the backfill. The total at-rest stress exerted on the wall could be the sum of the stresses due to gravity effects and the locked-in stresses due to densification. Fig. 2.9 shows the relationship between the extra coefficient due to locked-in stresses K_{ol} and the density change of soil. An empirical equation is proposed to estimate the K_o value for a compacted granular backfill as follows.

$$K_o = (1 - \sin\phi) + \left\{ \frac{\gamma_d}{\gamma_{d(\min)}} - 1 \right\} \times 5.5 \qquad (2.5)$$

where γ_d = actual compacted dry unit weight of soil behind the wall

$\gamma_{d(\min)}$ = dry unit weight of soil in the loosest state

It is obvious that the well-known Jaky's equation applies only when the backfill is deposited at its loosest state, and the method employed for backfill placement has a strong influence on K_o values.

2.2 Effects of Soil Compaction on Earth Pressure At-Rest

Compaction a soil can produce a stiff, settlement-free and less permeable mass. It is usually accomplished by mechanical means that cause the density of soil to increase. At the same time the air voids are reduced and. It has been realized that the compaction of the backfill material has an important effect on the earth pressure on the wall.

Several theories and analytical methods have been proposed to analyze the residual lateral earth pressures induced by soil compaction. Most of these theories introduce the idea that compaction represents a form of overconsolidation, where stresses resulting from a temporary or transient loading condition are retained following removal of this load.

2.2.1 Study of Rowe

Rowe (1954) conducted some experiments with cohesionless soils in shear-box and triaxial compression machines to investigate the influence of the confining stress, soil density, and strain history on soil behavior. Rowe proposed that compaction could be considered as the application and removal of a surficial surcharge pressure. Based on his test results, Rowe suggested that virtually all lateral soil stress induced by the surcharge loading would be retained after the surcharge removal. It is suggested that the coefficient of at-rest earth pressure following compaction could be expressed as $K_o{}'$.

$$K_o{}' = K_o\left(1 + \frac{\sigma_v + \Delta\sigma}{\sigma_v}\right) \tag{2.6}$$

where

K_o = the coefficient of earth pressure at-rest before compaction;

σ_v = the effective overburden pressure;

$\sigma_v + \Delta\sigma$ = the effective transient overburden pressure represent the peak loading during compaction process.

2.2.2 Study of Broms

Considering placement and compaction of horizontal layers of backfill adjacent to a non-deflection vertical wall, Broms (1971) proposed an analytical procedure based on the concept of hysteretic loading and unloading behavior. The stress path of hysteretic model that Broms' analytical procedure based is shown in Fig. 2.10a. Considering an element exists at some depth of the backfill, the initial stress state of the element can be illustrated as $\sigma_{hi} = K_o\sigma_{vi}$ which is shown at point A in Fig. 2.10. When the compactor is positioned immediately above the soil element, an increase of the vertical stress results in an increase in horizontal stress on the basis of the assumption of no lateral yield. The stress state can be expressed as $\sigma_{hm} = K_o\sigma_{vm}$ (point B). As the compactor moves off the fill, a subsequent decrease in vertical effective stress (unloading) results in no lateral stress decrease until a limitation (K_r-line) is reached (point C). The assumption is made that the maximum value of the horizontal stresses induced by compaction sustained until the vertical stress is reduced below a critical value at point C as shown in Fig. 2.10. After that, further unloading results in a decrease in horizontal stress through the stress path as $\sigma_{hf} = K_r\sigma_{vi}$ (point D) until the original vertical stress is reached. K_r is the coefficient of lateral earth pressure ($K_o \leq K_r \leq K_p$,

where K_p = coefficient of passive earth pressure). Broms (1971) assumed that K_r equals to $1/K_o$. Compared with the residual horizontal stress, σ_{hf} and initial horizontal stress, σ_{hi} at the same vertical effective stress. It is obviously that the σ_{hf} is much higher than σ_{hi}. The process of soil compaction would result in a higher residual horizontal stress exists.

For a deeper soil element, the vertical stress on the soil element increases under the roller load from A′ to B′, and upon unloading the full maximum horizontal load (σ_{hm}) is retained. Therefore, a critical depth z_c will exist, where the stress state after compaction will return exactly to point C′. The critical depth z_c can be expressed as follows:

$$z_c = \frac{K_o \sigma_{vm}}{\gamma K_r} \tag{2.7}$$

where $\sigma_{vm} = \gamma z + \Delta \sigma_v$, γz is the vertical stress due to the weight of soil, and $\Delta \sigma_v$ is the temporary increase in vertical stress at depth z due to the compactor.

Using the method proposed by Broms to calculate the compaction-induced earth pressure involves incremental analysis of the stresses resulting from the placement and compaction of each layer of backfill. Compaction at any point is modeled as the application of a transient increase in vertical effective stress ($\Delta \sigma_v$) caused by the compaction vehicle as determined by simple Boussinesq elastic analysis, followed by subsequent removal of the transient vertical load. The horizontal effective stresses due to the transient compaction loading, as well as those due to surcharge increases as a result of fill placement, are then determined by the model shown in Fig. 2.10.

Considering the effect of placing and removing a compactor at the surface of the fill, the distribution of lateral pressure due to compaction proposed by Broms (1971) is shown in Fig. 2.11 (a). Before compaction is applied to the fill, the soil element is under the condition of at-rest, and the horizontal pressure is equal to $K_o \sigma_v$ (curve 1). The application of the compactor leads to an increase in vertical stress which decreases with depth. The maximum horizontal pressure can be calculated with $K_o \sigma_{vm}$, where σ_{vm} equals to $\sigma_v + \Delta \sigma_v$ and $\Delta \sigma_v$ is the increase in vertical stress at any depth due to

the compactor (curve 2). As the compactor is removed, the backfill below the critical depth retains the increased horizontal stress and the fill above the critical depth reduces its horizontal stress to $K_r\sigma_v$ (curve 3). Based on the above discussions, as the backfill is compacted at the surface, the profile of the pressure distribution is indicated by the shaded area in Fig. 2.11 (a).

In reality, compaction is carried out regularly on thin layers of fill up the back of the retaining wall. The residual lateral pressure distribution is then given by the locus of the point A as the surface of the fill moves upward. A simplified distribution is illustrated in Fig. 2.11 (b).

2.2.3 Study of Peck and Mesri

Based on the elastic analysis, Peck and Mesri (1987) presented a calculation method to evaluate the compaction-induced earth pressure. The lateral pressure profile can be determined by four conditions on σ_h, as illustrated in Fig. 2.12 and summarized in the following.

1. Lateral pressure resulting from the overburden of the compacted backfill,

$$\sigma_h = (1 - \sin\phi)\gamma z \qquad (2.8)$$

2. Lateral pressure limited by passive failure condition,

$$\sigma_h = \tan^2(45 + \phi/2)\gamma z \qquad (2.9)$$

3. Lateral pressure resulting from backfill overburden plus the residual horizontal stresses,

$$\sigma_h = (1 - \sin\phi)\gamma z + \frac{1}{4}(5^{1.2\sin\phi} - 1)\Delta\sigma_h \qquad (2.10)$$

where $\Delta\sigma_h$ is the lateral earth pressure increase resulted from the surface compaction loading of the last backfill lift and can be determined based on the elastic solution.

4. Lateral pressure profile defined by a line which envelops the residual lateral pressures resulting from the compaction of individual backfill lifts. This line can be computed by Eq. 2.11.

$$\frac{\Delta\sigma_h}{\Delta z} = \frac{1-\sin\phi}{4}(5-5^{1.2\sin\phi})\gamma \tag{2.11}$$

Fig. 2.12 indicates that near the surface of backfill, from point a to b, the lateral pressure on the wall is subject to the passive failure condition. From b to c, the overburden and compaction-induced lateral pressure profile is determined by Eq. 2.10 From c the lateral pressure increases with depth according to Eq. 2.11 until point d is reached. Below d, the overburden pressure exceeds the peak increase in stress by compaction. In the lower part of the backfill, the lateral pressure is directly related to the effective overburden pressure.
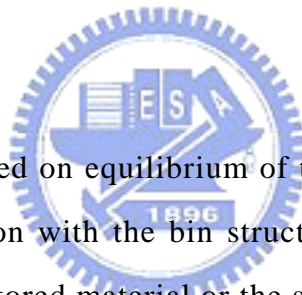
2.3.4 Study of Chen

Chen (2002) reported some experiments in non-yielding retaining wall at National Chiao Tung University to investigate influence of earth pressure due to vibratory compaction. Air-dry Ottawa sand was used as backfill material. Vertical and horizontal stresses in the soil mass were measured in loose and compacted sand. Based on his test results, Chen (2002) proposed four points of view: (1) the compaction process does not result in any residual stress in the vertical direction. The effects of vibratory compaction on the vertical overburden pressure are insignificantly, as indicated in Fig. 2.13 and Fig. 2.15; (2) after compaction, the lateral stress measured near the top of backfill is almost identical to the passive earth pressure estimated with Rankine theory (Fig. 2.14). The compaction-influenced zone rises with rising compaction surface. Below the compaction-influenced zone, the horizontal stresses converge to the earth pressure at-rest, as indicated in Fig. 2.14(e); (3) when total (static + dynamic) loading due to the vibratory compacting equipment exceeds

the bearing capacity of foundation soils, the mechanism of vibratory compaction on soil can be described with the bearing capacity failure of foundation soils; (4) the vibratory compaction on top of the backfill transmits elastic waves through soil elements continuously. For soils below the compaction-influenced zone, soil particles are vibrated. The passive state of stress among particles is disturbed. The horizontal stresses among soil particles readjust under the application of a uniform overburden pressure and constrained lateral deformation, and eventually converge to the at-rest state of stress.

2.3 Methods to Estimate Lateral Pressure on Silos and Bunkers

These methods are based on equilibrium of the stored material in a static condition. Elastic interaction with the bin structure is not considered, nor is strain energy in either the stored material or the structure.

2.3.1 Janssen's Method

Janssen's method (1895) reported silo equation to estimate the distribution of the horizontal pressure with stored material as shown in Fig. 2.16. Equating the vertical forces to zero gives:

$$qA + \gamma A dy = A\left[q + dy\frac{dq}{dy}\right] + \mu' p(Udy) \qquad (2.12)$$

where

q = static vertical pressure at depth Y

A = area of horizontal cross section through the silo

U = perimeter of horizontal cross section

p = pressure of stored material against walls at depth Y below surface of stored
material

$\mu' = \tan \delta$ = coefficient of friction between stored material and wall

γ = unit weight of stored material

Substituting kq for p, and "hydraulic radius" R for A/U, the differential equation of equilibrium becomes:

$$dq/dy = \gamma - \frac{\mu' k}{R} q \qquad (2.13)$$

where k is the ratio of horizontal pressure to vertical.

The solution to this differential equation is the Janssen formula for vertical pressure at depth Y:

$$q = \frac{\gamma R}{\mu' k}\left[1 - e^{-\mu' k Y / R}\right] \qquad (2.14)$$

Hence, to compute the horizontal pressure p, Eq. 2.14 is multiplied by k. Thus, the Janssen's (1895) equation for horizontal pressure is:

$$p = \frac{\gamma R}{\mu'}\left[1 - e^{-\mu' k Y / R}\right] \qquad (2.15)$$

The above derivation makes no assumption as to shape of the silo cross section. If the cross section is rectangular with side lengths a and b will have different pressures on short and long sides. A common procedure is to let $R = a'/4$ when computing pressure on the long side b, where:

$$a' = \frac{2ab}{a+b} \qquad (2.16)$$

An alternate value of a' suggested by Reimbert is to use

$$a' = \frac{2ab - a^2}{b} \qquad (2.17)$$

2.3.2 Reimbert and Reimbert's Method

In 1953 and 1954, Marcel and Andre Reimbert presented their method for computing static pressure due to stored material. Their derivation recognizes that at large depths Y, the curve of lateral pressure becomes asymptotic to the vertical axis. (This can be shown by plotting pressures given by the Janssen equation or by noting that for large Y-values, the first derivative, dp/dy, approaches zero.) At that depth, the lateral pressure reaches a maximum, shown as p_{max} on Fig. 2.17 (a). A lamina of material at this depth shows in Fig. 2.17 (b). It has equal vertical pressure above and below. Consequently, the lamina weight is exactly balanced by wall friction, or:

$$\gamma A dy = \mu' p_{max} U dy \qquad (2.18)$$

Thus:

$$p_{max} = \gamma R / \mu' \qquad (2.19)$$

where R is the hydraulic radius, A/U.

The Reimbert equation for lateral static pressure at depth Y is:

$$p = p_{max} \left[1 - \left(\frac{Y}{C} + 1 \right)^{-2} \right] \qquad (2.20)$$

For rectangular silos with short side and long side b, p_{max} and C on the longer

wall are as follows:

$$p_{max} = \gamma a'/4\mu' \qquad (2.21)$$

$$C = \frac{a'}{\pi\mu'k} \qquad (2.22)$$

where $a' = \dfrac{2ab - a^2}{b}$.

2.3.3 Spangler and Handy's Method

Fig. 2.18 represents a section of a ditch conduit 1 unit in length. Considering a thin horizontal element of the fill material of height dh located at any depth h below the ground surface. Equating the upward and downward vertical forces on the element, the following equation is obtained.

$$V + dV + 2K\mu'\frac{V}{B_d}dh = V + \gamma B_d dh \qquad (2.23)$$

where

V = vertical force on the top of the element

$V + dV$ = vertical force on the bottom of the element

$\gamma B_d dh$ = weight of the fill element

$K(V/B_d)dh$ = the lateral force on each side of the element, it is assumed that the vertical pressure on the element is uniformly distributed over the width B_d. Since the element has a tendency to move downward in relation to the sides of the ditch, these lateral pressures induce upward shearing forces equal to $K\mu'(V/B_d)dh$.
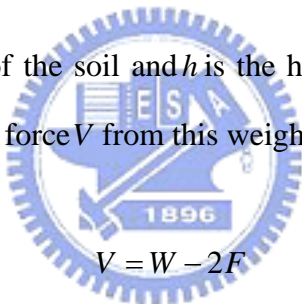
Eq. 2.23 is a linear differential equation, the solution for V is:

15

$$V = \gamma B_d^2 \frac{1 - e^{-2K\mu'(h/B_d)}}{2K\mu'} \tag{2.24}$$

Fig. 2.19 (a) shows some retaining walls are built in front of a stable rock face, not so much to retain soil as to prevent rockfalls. Granular backfill placed in the relatively narrow gap between the wall and the natural outcrop is partly supported by friction on each side, from the wall and form the outcrop. Since the friction is distributed vertically it reduces vertical stress within the soil mass, which in turn reduces the horizontal stress and the overturning moment. The weight of W of a soil prism between the wall and the rock face parallel to the wall and at a distance B from the wall (Fig. 2.19 (a)) is:

$$W = \gamma Bh \tag{2.25}$$

where γ is the unit weight of the soil and h is the height down from the top of the wall. The vertical unsupported force V from this weight is:

$$V = W - 2F \tag{2.26}$$

where F is the vertical component of wall friction. The vertical stress at any height h is $\sigma_v = V/B$, and the horizontal stress is:

$$\sigma_h = K\frac{V}{B} \tag{2.27}$$

where K is the coefficient of Lateral earth pressure. Substitution for V from Eq. 2.24, gives:

$$\sigma_h = \frac{\gamma B}{2\mu}\left[1 - e^{-2K\mu(h/B)}\right] \tag{2.28}$$

16

where $\mu = \tan\delta$, the coefficient of friction between the soil and the wall.

Some solutions of Eq. 2.28 for different values of B are shown in Fig. 2.19 (b). It can be seen that the soil pressure, instead of continuing to increase with increasing values of h, level off at a maximum value defined by Eq. 2.28 when When h approaches ,

$$\sigma_{max} = \frac{\gamma B}{2\mu} = \frac{\gamma B}{2\tan\delta} \qquad (2.29)$$

2.3.4 Frydman and Keissar's Study

Frydman and Keissar (1987) used the centrifuge modeling technique to test a small model wall, and changes in pressure from the at-rest to the active condition was observed. The centrifuge system has a mean radius of 1.5 m, and can develop a maximum acceleration of 100 g, where g is acceleration due to gravity. The models are built in an aluminum box of inside dimensions 327 × 210 × 100 mm. Each model includes a retaining wall made from aluminum (195 mm high × 100 mm wide × 20 mm thick) as shown in Fig. 2.20. The rock face is modeled by a wooden block, which can, through a screw arrangement, be positioned at varying distances d from the wall. Face of the block is coated with the sand used as fill, so that the friction between the rock and the fill is equal to the angle of internal friction of the fill. Frydman and Keissar (1987) found that Spangler and Handy's solution may be used for estimating lateral pressure for the no-movement (K_o) condition.